Available online at www.sciencedirect.com

ScienceDirect

Energy Procedia 00 (2015) 000–000

Energy Procedia

www.elsevier.com/locate/procedia

International Conference on Concentrating Solar Power and Chemical Energy Systems, SolarPACES 2014

Transient models and characteristics of once-through line focus systems

Jan Fabian Feldhoff[a]*, Tobias Hirsch[a] , Robert Pitz-Paal[b], Loreto Valenzuela[c]

[a]*DLR, Institute of Solar Research, Wankelstrasse 5, 70563 Stuttgart,Germany*
[b]*DLR, Institute of Solar Research, Linder Hoehe, 51147 Cologne,Germany*
[c]*CIEMAT-PSA, Plataforma Solar de Almería, 04200 Tabernas, Almería, Spain*

Abstract

A transient model is the basis for understanding the characteristics of dynamic systems. It must always be a tradeoff between (modeling and computational) effort and the desired output. Thus, it is necessary for complex systems to develop special models adapted to the purpose. This has been performed for the case of direct steam generation (DSG) in parabolic trough or linear Fresnel solar fields, in which there is a long section of two-phase flow. In the once-through mode (OTM), feed water from the power block is directed to the inlet of a loop. The water is then preheated, completely evaporated and superheated along the loop. This paper presents two different types of transient models for such systems.
A discretized finite element model is used for detailed system characteristics and understanding. A second moving boundary model is developed which includes the combination of lumped parameters with distributed information. This fast model can especially be used for control studies and model based predictive controllers. Both models are compared against experimental data and differences regarding various system characteristics are shown. Further models like linear transfer functions in the time-domain are mentioned and an overall overview on transient DSG models is provided.

Peer review by the scientific conference committee of SolarPACES 2014 under responsibility of PSE AG.

Keywords: transient modeling, moving boundary model, direct steam generation, solar-thermal once-through boiler, parabolic trough.

* Corresponding author. Tel.: +49 711 6862-362; fax: +49 711 6862-8032.
E-mail address: jan.feldhoff@dlr.de

Peer review by the scientific conference committee of SolarPACES 2014 under responsibility of PSE AG.

Nomenclature

DISS	Direct Solar Steam (European research project and name of test facility at PSA)
DFEM	Discretized finite element model
DLR	German Aerospace Center
DSG	Direct steam generation
EPE	End (point) of evaporation
LTI	Linear, time-invariant (parameter model)
MBM	Moving boundary model
OTM	Once-through mode
PDE	partial differential equations
PSA	Plataforma Solar der Almería in Spain

Variables

a	empirical constant for heat loss	α	heat transfer coefficient [W/m²/K]
A	cross section area [m²]	γ_h	derivative of density over enthalpy at constant pressure [kg*s²/m^5]
c	specific heat capacity [J/kg/K]		
d	diameter [m]	γ_p	derivative of density over pressure at constant enthalpy [s²/m²]
F_R	frictional length-specific pressure loss [Pa/m]		
G_{eff}	effective incoming solar heat flux [W/m²]	λ	thermal conductivity [W/m/K]
h	specific enthalpy [J/kg]	ρ	density [kg/m³]
l	length [m]	ζ	pressure drop coefficient [-]
$\dot{m}$	mass flow [kg/s]	ϑ	temperature [°C]
p	pressure [Pa]	η_{opt}	optical efficiency at certain time instant [-]
Q	convective heat flow to the fluid [W]		
q_L	length-specific convective heat flow to the fluid [W/m]		
$q_{abs,L}$	length-specific absorbed heat from solar input [W/m]		
$q_{loss,L}$	length-specific heat loss [W/m]		
t	time [s]		
u	internal energy [J/kg]	**Indices**	
V	volume [m³]	i	inner
w	fluid velocity [m/s]	w	tube wall
w_{ap}	collector aperture width [m]	L	length-specific
z	length coordinate along loop [m]	o	outer

1. Introduction

Models can be used to reproduce experimental data, study system behavior, predict future behavior, or develop suitable control concepts. One could imagine that models become more valuable with the complexity of the system and the accuracy of the results. Though this is true in general, a good model must always be a tradeoff between (modeling and computational) effort and the desired simulation result. Thus, it is necessary for complex systems to develop special models adapted to the desired purpose. While modeling of single-phase fluid behavior in parabolic troughs is rather simple, the case of direct steam generation (DSG) is more complex. This is due to a long section of two-phase flow and a large density difference of the fluid between inlet and outlet of a loop. In once-through mode (OTM), feed water from the power block is directed to the loop inlet of a parabolic trough or linear Fresnel row. The water is then preheated, completely evaporated and superheated along the loop. The superheated steam is used to run a steam turbine and generate electricity. The OTM is a current field of research [1] with high interest of industry in order to reduce the levelized cost of electricity in solar thermal power plants.

This paper provides a general overview of transient OTM modeling and then presents two different types of OTM models each tailored to a particular application purpose. First, DLR's most accurate transient model is described. It is based on a discretized finite volume approach which considers transient energy and mass balance, static momentum balance, and thermodynamic phase-equilibrium in the two-phase flow region [2]. Second, the moving boundary model theory for steam generators [3-6] is extended to meet the boundary conditions of the OTM in line focus solar systems. Both models are validated against experimental data from the new DISS test facility at the Plataforma Solar de Almería (PSA), Spain [7, 8]. The plant is a flexible DSG test loop with parabolic troughs, a total length of 1000 m and outlet steam parameters of up to 500°C and 110 bars [9]. In order to provide more detailed insight into the system behavior, additional simulations are shown and the difference between the models is depicted. Special emphasis is placed on the non-minimum phase behavior during disturbances at the loop inlet.

2. Modeling

2.1. General overview on model approaches

Various model approaches for the DSG process –or steam generation in general– exist. They can be distinguished predominantly by the way the two-phase flow is considered in the derivation of the main equations. The model must consider that at the inlet a first part of the collector will preheat the water, such that we have liquid single-phase flow with a low dependency on pressure. Then we have two-phase flow in the evaporation part followed by single-phase flow in the superheating part, both depending significantly on fluid pressure.

Complex models developed for nuclear industry consider the flow by a 6-equation model: mass, momentum and energy balance equations are stated for each phase separately. The equations are then closed by mainly empirical interaction laws [10]. Simulation tools like CATHARE [11], ATHLET [12] or RELAP5 [13] use such models for steam generation. ATHLET is currently adapted also for the simulation of the DSG process in parabolic troughs as considered here [14]. The drawback of these models is that the empirical interaction laws usually are not known and require a considerable effort to be derived. However, if available, these models could offer a very deep insight into local flow phenomena. Since the aim of this paper is rather to put emphasis on the overall system dynamics, such detailed models are not considered in this paper any further. A good introduction can be found in [14].

The model equations can be significantly simplified, if we assume that the two-phase flow can be considered as a homogeneous fluid, i.e. liquid and steam are in thermodynamic equilibrium, have the same velocity and are distributed equally within a cross section. Lippke [15] uses such a model with mass and energy balances for the homogeneous fluid. As described in [16], the pressure –or impulse balance, respectively– is updated in a separate iteration step based on static pressure loss correlations. Steinmann [17] developed a model based on transient mass, energy and momentum balances. The finite difference model uses the method of characteristics for solving the boundary conditions at the discretization bounds. Even very fast dynamics can be simulated well with this model due to the non-steady momentum balance. Hirsch [18] then derived the mass and energy balances as explicit functions of enthalpy and pressure to simulate the DSG process. The programming language Modelica and its Dymola interface are used [2]. The momentum balance is incorporated by an inverse steady pressure loss correlation. The outlet pressure, inlet mass flow and inlet enthalpy are the main boundary conditions. This model is used in this paper for system studies and is described in the next section.

A model based on similar equations has been implemented in commercial computational fluid dynamics software by Lobón [19]. This tool allows the combined modeling of fluid dynamics and thermo-mechanical behavior of the pipes. However, computation times are very high and take more than 100 times longer than a comparable simulation with the Hirsch/Dymola model (compared to estimations given in [19]), which complicates the practical application. If the mechanical stress is to be analyzed either such a tool can be used or the simulations can be performed in two separate steps. At first, the faster model (e.g. by [2]) is used to generate the dynamic fluid behavior and to identify critical locations. Then, in a second step, only the critical part is simulated by a mechanical analysis tool with the boundary conditions of the first simulation.

Further simplification can be achieved, if the distributed character of the system is ignored. The boiler is then divided into three sections, namely preheating, evaporation, and superheating. Only the main mass and energy balances are considered for these sections. The state of the system can then predominantly be characterized by the

lengths of the different sections. These lengths or control volume boundaries, respectively, can vary in a transient model and led to the name *moving boundary model* (MBM) theory. One of the first papers using this MBM approach for steam generators was the one by Adams [20]. Ray then used MBM theory for modeling nuclear [4] and solar [21] boilers. Jensen [22, 23] later on assessed various MBM cases for two-phase flow refrigeration systems. Depending on the inlet and outlet conditions of the fluid (e.g. liquid, two-phase, or gas flow at the outlet), different MBM formulations are suggested –and implemented in Modelica. The difference to the work of Ray is in the characterization of two-phase flow. While Ray uses the thermodynamic approach of internal energy, Jensen follows the approach of mean void fraction, which can also consider slip, i.e. the velocity ratio of gas and liquid flow within a cross section. The latter approach has lately been used by Zapata [6] for the simulation of a parabolic dish steam engine and by Bonilla [3] for OTM in parabolic troughs. The latter paper validates the MBM against experimental data from the old DISS test facility of 500 m length. As contribute to Ray and due to the rather empirical character of the mean void fraction, the MBM presented in this paper is based on the work of Ray [21]. MBM formulations usually aim at fast simulations to catch the main dynamics of a system and are thus used for control purposes. A pure lumped model then only offers information about the boundaries and outlet variables, e.g. outlet enthalpy/temperature of the loop in our case. Note, that the end point of evaporation (EPE) is explicitly modeled, which is not the case for discretized models. As it is an interesting variable for OTM analysis, this is a clear advantage of MBMs. Advanced OTM concepts [7], however, consider using one or two injectors within the collectors' loop, such that information before those injectors is desired, too. The MBM formulation has thus been extended to consider injections in the evaporation as well as in the superheating section. The adapted formulations are described below in this paper and model results are presented. It is now possible to get fast information e.g. about the temperature before the superheating injection, which can then be used as additional variable for model-based control or for non-linear state estimation.

In classical control theory, the transient dependencies are usually described in the form of linear, time-invariant (LTI) transfer functions or state space models. Ideally, they can be derived from first principles by stating the non-linear equations and linearizing them around the desired operating point. Control theory then offers various ways of designing appropriate controllers, e.g. by rule-of-thumb correlations, pole placement or internal model control [24]. During the development of fossil and nuclear boilers, many papers and books have been dedicated to control and, in consequence, to deriving suitable models. One of the first books deriving first principle models for steam generators was the one by Profos [25]. Besides many follow-up works, it has been the basis for the development of LTI transfer functions for DSG in parabolic troughs by Eck [26]. Eck adapted the LTI models for the superheating section to the needs of line focus systems. This is summarized in English in [27]. It can be shown that the predominant, transcendent temperature transfer function is equivalent to the one used for single-phase compressible fluids. This transcendent term accounts for heat capacity and heat transfer effects between inlet and outlet temperature. Due to greater wall thickness (amongst others), the approximation of this term is an n-th order (PT_n) element [27] for superheater sections, while a first order (PT_1) element [28] is sufficient for single-phase fluids. Eck [26] also derived LTI models for the evaporation section in the frequency-domain. Both can serve for classical controller design. The drawback of the evaporator models, however, is that they are not numerically stable in the time-domain and, thus, cannot be used for model-based predictive controllers.

An alternative to these first principles LTI models is to derive time-domain models from other simulations or experimental data. Valenzuela [29-31] identified the most relevant LTI transfer functions to control the DSG process at the old DISS test facility and demonstrated the derived classical controllers for recirculation mode and once-through mode. This approach is recommended so far, as a complete LTI description for OTM based on first principles is still lacking. Thus, the discretized model (e.g. as presented in the next section) can be used to derive the desired transfer functions by choosing a suitable structure and identifying the parameters depending on the operating point. One can use the results of Eck [26] to verify this approach: the order of the LTI transfer function mainly depends on the collector dimensions, whereas the parameters (time constant and gain) highly depend on the operating point.

With the two model approaches presented in the next sections, the whole range of model applications can be covered or derived. A comparison is made in the next chapter.

2.2. Discretized finite element approach

The mass, energy and impulse balance for a unidirectional fluid flow can be written as [2, 26]:

$$\frac{\partial \rho}{\partial t} + \frac{\partial (\rho w)}{\partial z} = 0 \tag{1}$$

$$\frac{\partial (\rho u)}{\partial t} + \frac{\partial (\rho w h)}{\partial z} = \frac{Q}{V} \tag{2}$$

$$\frac{\partial (\rho w)}{\partial t} + \frac{\partial (\rho w^2)}{\partial z} + \frac{\partial p}{\partial z} + \zeta \frac{\rho w^2}{2d} = 0 \tag{3}$$

These equations include density ρ, fluid velocity w, internal energy u, enthalpy h, pressure p, pressure drop coefficient ζ, diameter d and convective heat flow to the fluid Q per volume V. The equations form a set of partial differential equations (PDE) with derivatives of time t and location z.

The non-steady momentum balance can be approximated by a stationary frictional pressure loss correlation [2]:

$$\frac{\partial p}{\partial z} = F_R \tag{4}$$

By applying the definition of enthalpy ($h = u + p/\rho$) and equation (1), equation (2) simplifies to

$$\rho \frac{\partial h}{\partial t} + \rho w \frac{\partial h}{\partial z} - \frac{\partial p}{\partial t} = \frac{Q}{V} \tag{5}$$

The equations above are valid for single-phase flow as well as for the homogeneous equilibrium two-phase flow assumption. Water/steam properties can be calculated uniquely from the two properties pressure and enthalpy in the complete range from loop inlet to outlet. It is thus straight forward to use pressure and enthalpy as the state variables for the fluid. We further introduce the fluid properties γ_p and γ_h:

$$\rho = \rho(p,h); \quad \gamma_p = \left.\frac{\partial \rho}{\partial p}\right|_h; \quad \gamma_h = \left.\frac{\partial \rho}{\partial h}\right|_p \tag{6}$$

Equations (1), (5), and (6) are now used to explicitly formulate the time derivatives of enthalpy and pressure. For further simplification we assume that the pressure variation in time is negligible for the energy balance. The resulting PDE set is

$$\frac{\partial h}{\partial t} = \frac{1}{\gamma_p}\left(\frac{\gamma_p h}{\rho A}\frac{\partial \dot{m}}{\partial z} - \frac{\gamma_p}{\rho A}\frac{\partial (h\dot{m})}{\partial z} - \frac{\gamma_p}{\rho V} Q\right) \tag{7}$$

$$\frac{\partial p}{\partial t} = \frac{1}{\gamma_p}\left(-\frac{\gamma_h h + \rho}{\rho A}\frac{\partial \dot{m}}{\partial z} - \frac{\gamma_h}{\rho A}\frac{\partial (h\dot{m})}{\partial z} - \frac{\gamma_h}{\rho V} Q\right) \tag{8}$$

Note that γ_p is only introduced in equation (7) to show the similarity to equation (8). An important aspect for choosing the state combination of p and h is the resulting de-coupled set of equations, which now becomes visible. Though Modelica supports implicit formulation, the decoupling and the explicit formulation of states significantly improve the numerical stability. The partial derivatives in space can now be replaced by an upwind discretization or similar scheme. The dependencies for a simple upwind scheme as described in [2] are then

$$\frac{\partial h}{\partial t} = \frac{\partial h}{\partial t}(h^i, h^{i-1}, p^i, Q^i, \dot{m}^i, \dot{m}^{i-1}) \tag{9}$$

$$\frac{\partial p}{\partial t} = \frac{\partial p}{\partial t}(h^i, h^{i-1}, p^i, Q^i, \dot{m}^i, \dot{m}^{i-1}) \tag{10}$$

$$\dot{m}^i = \dot{m}^i(p^i, p^{i+1}, h^i) \tag{11}$$

Note that for fast simulations an explicit pressure loss equation like [32] should be inverted to solve equation (11). The mass flow values in equations (9) and (10) can then be replaced.

As the thermal inertia of the pipes and receivers plays a decisive role in line focus systems, the change of the tube temperature must be modeled as well. A simple approach is used which neglects axial heat conduction and temperature gradients within a cross section. The transient heat balance for the tube wall can then be formulated as

$$\frac{\partial \vartheta_w}{\partial t} = \frac{1}{\rho_w A_w c_w}\left(q_{abs,L} - q_{loss,L} - q_L\right) \tag{12}$$

This includes wall temperature ϑ_w, wall density ρ_w, wall cross section A_w, wall heat capacity c_w as well as the length-specific absorbed heat from solar input $q_{abs,L}$, heat loss $q_{loss,L}$, and thermal power to the fluid q_L.

The absorbed heat by the receiver can be interpreted as effective incident heat to the receiver tube. It can be calculated with the direct normal irradiance (DNI) to the collector corrected by various optical factors. These are incidence angle modifier (IAM), cosine of the incidence angle, cleanliness of the mirrors, optical peak efficiency of the collector and various other factors. As they are not relevant for the main dynamic behavior of the system, we consider the heat input by the following simple formulation:

$$q_{abs,L} = w_{ap}\, DNI(t)\, \eta_{opt}(t) = w_{ap}\, G_{eff}(t) = \frac{Q_{abs}}{\Delta z} \tag{13}$$

The *DNI* is corrected by a time (and by that also incidence angle) dependent factor η_{opt}. This gives the effective incoming solar heat flux G_{eff}. The multiplication with the aperture width w_{ap} of the collector gives the length-specific heat input, e.g. per element length Δz. If *DNI* is known, $q_{abs,L}$ is also known.

The heat loss per length can be calculated by detailed models, e.g. [33], or by empirical correlations for the receivers. We use the correlation as described in [9] with coefficients for the new receivers at the DISS test facility taken from experiments (temperatures in °C, heat loss in W/m):

$$q_{loss,L} = a_1\vartheta_w + a_4\vartheta_w^4 = 0.16155\,\frac{W}{m\cdot°C}\,\vartheta_w + 6.4407\cdot 10^{-9}\,\frac{W}{m\cdot°C^4}\,\vartheta_w^4 \tag{14}$$

The heat input to the fluid can be calculated assuming the mean wall temperature ϑ_w, inner and outer diameter of the receiver d_i and d_o, thermal conductivity of the tube wall λ_w, fluid temperature ϑ, and heat transfer coefficient α.

$$q_L = \frac{\pi}{\frac{1}{d_i\alpha} + \frac{1}{2\lambda_w} ln\left(\frac{d_i+d_o}{2d_i}\right)}\left(\vartheta_w - \vartheta\right) \tag{15}$$

For single-phase flow, the correlations of Gnielinski [34] or Dittus/Boelter [35] can be used. For two-phase flow, approaches from [36-39] and others can be used as summarized in [40]. However, the heat transfer coefficient is very high and thus the influence on the prevailing time constant for heat transfer is low [18]. Therefore, the heat transfer coefficient in two-phase flow can usually be assumed constant for our purposes, e.g. in the range of 10 kW/m²/K. In the results presented we have used the correlations by [37].

Summing up, each element has the three states h^i, p^i and $\vartheta_w{}^i$. Due to the used discretization, the terminal constraints are the mass flow and enthalpy at the collector inlet and the pressure at the collector outlet.

2.3. Moving boundary model approach

The model of Ray [4, 21] is used as basis for the extended moving boundary model (MBM) approach derived here. A schematic diagram of the original boundaries and sub-volumes adapted to a parabolic trough loop is given in Figure 1a. The boundaries and volumes are enumerated consecutively. 1 denotes the inlet of the boiler, 2 is the preheating section, 3 is the boundary between liquid and two-phase flow (or the initial location of boiling,

respectively), 4 is the evaporation section, 5 denotes the boundary between two-phase and pure steam flow (or EPE), 6 is the superheater section, and 7 represents the outlet of the solar boiler. The advantage of this model is its simplicity, the speed of computation and the explicit modeling of the EPE defined as length l_{15}.

In the original Ray model, there is no injection of water foreseen. For current systems under research up to two injections are considered for a high control quality [7]. A nominal operating point with two injections (see Fig. 1b) would have one injector in the evaporation zone (A) and one injector in the superheating zone (B). If we want to derive information before those injectors, the MBM must foresee them as well. We can interpret this as modeling three MBMs for the three fixed distances/sub-systems 1-A, A-B, and B-7. The evaporation section is divided into the control volumes 4I and 4II, and so is the evaporation section (6II and 6III). This model is called our *base* model.

The model equations for this base model have been derived using mass and energy conservation and have been applied to the DISS test facility by Morille [41]. It consists of 14 system state variables, which represent the volumes or boundaries of the model. These are the wall temperatures ϑ_w and specific internal energies u of each of the five volumes (2, 4I, 4II, 6II, 6III), the start and end of boiling (l_{13} and l_{15}) as well as the density of the saturated steam (ρ_5). As the pressure drop along the loop can be significant, the pressure at injection A (p_A) is also introduced as state –which is another significant difference to [23]. The pressure at the outlet (p_7) is a simulation input and known. If only those states were accounted for in the model, changes in the input would immediately take effect on the outlet conditions –bearing in mind that it is a lumped and not a distributed representation of the loop. For example, an increase in inlet mass flow would result in an immediate drop in outlet temperature. The real system has significant delay and, therefore, this has to be considered in the model as well. Thus, 13 intermediate state variables for delaying the inputs are added in our model. These are the input mass flows and enthalpies (inlet, injection A, injection B) and the solar heat input for each volume. Due to the long response of the system to changes in the inlet mass flow, this input is delayed by a second order approximation, while all other intermediate states are of first order. Note, that Ray [21] uses the same delay for the inlet enthalpy, but none for the other inputs. As a result, we obtain a system of 27 non-linear differential equations combined with additional algebraic equations, mainly correlations for thermo-physical properties of water/steam.

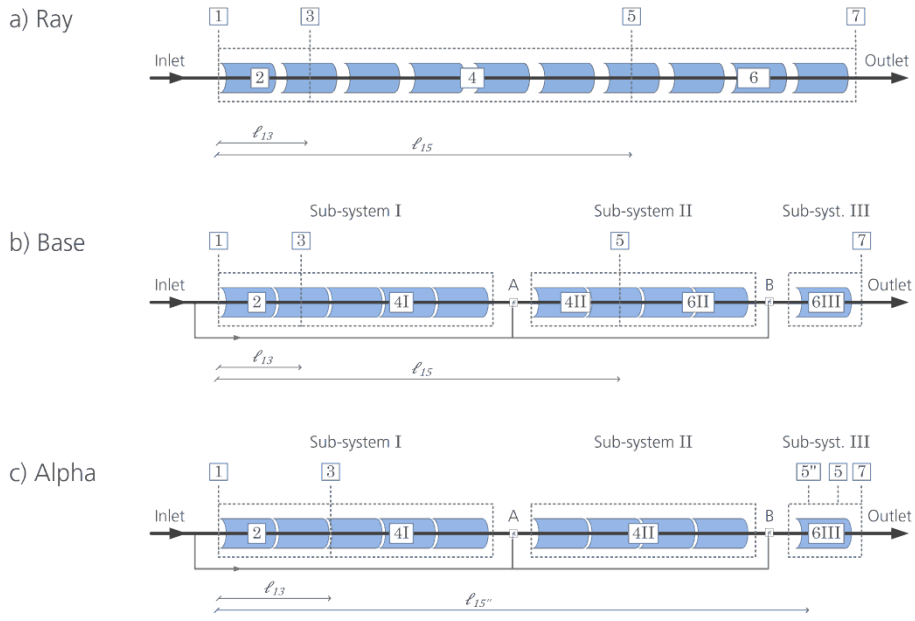

Fig. 1. Boundaries (1,3,5,7) and control volumes (2,4,6) of the moving boundary models for a parabolic trough loop with two injectors (A, B).

The main difference to the model of Ray [21] is the injector A in the evaporation section and, in consequence, the determination of the derivative of the length l_{15}. The Ray model [21] suggests

$$\frac{dl_{15}}{dt} = \frac{\dot{m}_3(h_3-u_4)-\dot{m}_5(h_5-u_4)+q_{L4}l_{35}-l_{35}A\rho_4\frac{du_4}{dt}+\rho_3A(h_3-u_4)\frac{dl_{13}}{dt}}{\rho_5A(u_4-h_5)} \tag{16}$$

Volume 4 is separated in the base model such that the derivative can be calculated now by

$$\frac{dl_{15}}{dt} = \frac{\dot{m}_{II,in}(h_{II,in}-u_{4II})-\dot{m}_5(h_5-u_{4II})+q_{L4II}l_{A5}-l_{A5}A\rho_{4II}\frac{du_{4II}}{dt}}{\rho_5A(u_{4II}-h_5)} \tag{17}$$

The subscript 'II,in' indicates variables at the inlet to sub-system II after mixture with injection A. Instead of the derivative of l_{13} we now have an influence of the derivative of internal energy of the volume 4II (u_{4II}). The time derivative of the internal energies of volumes 4I and 4II are

$$\frac{du_{4I}}{dt} = \frac{1}{l_{3A}\rho_{4I}A}\left(\dot{m}_3(h_3-u_{4I})-\dot{m}_{I,out}\left(h_{I,out}-u_{4I}\right)+q_{L4II}l_{3A}-\rho_3A(h_3-u_{4I})\frac{dl_{13}}{dt}\right) \tag{18}$$

$$\frac{du_{4II}}{dt} = \frac{1}{2}(h_{II,in}+h_5) \tag{19}$$

Note that u_{4II} is only a rough assumption to get an update of l_{15} as it neglects changes in solar input. This is considered in the 'real' evolving state ρ_{4II} as is presented analogously in [4]. Assumption (19) is used to de-couple the calculation of the state in volume 4II and l_{15}. The two superheating sections 6II and 6III in the base model are calculated analogous to the original approach as well. Internal energies are used as states and the outlet boundaries are calculated by extrapolation.

If strong disturbances occur, e.g. when irradiation is too low or the mass flows are too high, we might still have two-phase flow at or after injector B. In this case, the MBM base formulation is not valid any more, as the control volume 6II would vanish. Thus, we have to use a different MBM formulation and switch between those formulations. The resulting MBM formulation is called *alpha* model here and is shown in Fig. 1c. During switching and due to the injection of additional water, the boundary l_{15} will jump from L_{1B} to a location downstream of sub-system III (indicated as 5 in Fig. 1c). Before switching, the real system would even have two end points of evaporation: one before injection B, from which the steam is slightly superheated, and one after injector B, as the superheated steam is cooled down to wet steam before it is heated in sub-system III again. One way for switching is shown in [3]. However, we want to keep the same states as in the base model formulation for computational simplification. Therefore, we keep the l_{15} definition of the base model, which suggests the length to point 5" (see Fig. 1c). The internal energy u_{6III} and the inlet enthalpy of sub-section III ($h_{III,in}$) are now calculated by interpolation between A and 5". All of the remaining states and formulations of the alpha model can be evolved by the same equations as in the base model which reduces the switching effort to a minimum.

Comparing the MBM to the discretized model shows that we have only 27 states instead of about 600 (3 states/element*200 elements/loop). The computation time of the MBM is only about 1/1000 of the DFEM.

3. Validation of models and characterization

The models presented in the former chapter have limited application ranges. The discretized finite element model (DFEM) is valid for the complete range of DSG solar field, for single collectors and whole loops, for water, steam and two-phase flow. The moving boundary model (MBM) is restricted to its original configuration, i.e. a complete loop with two-phase flow or superheated steam at the outlet.

Validation is performed with experiments at the new DISS test facility [7] in once-through mode of which a schematic diagram is shown in Fig. 2. Note that the loop configuration is special in the sense that we have additional crossover piping between collectors #1B and #1, #8 and #9, as well as between #11 and #12. This piping causes additional delay in the loop which would not be present in a commercial loop. To consider this in the DFEM, we must model the additional piping. For verification we use single-phase flow through the complete loop, focus and defocus some collectors and compare the data to the model. This is shown in Fig. 3. The DFEM input used is the data of loop inlet mass flow, loop inlet temperature, DNI, and focus signals (0 or 1) of each collector. For the

1000 m loop, the single-phase flow is modeled very well. As a side effect, we can easily apply this model also for systems using oil or molten salts as heat transfer fluid in the solar field, by just changing the fluid property functions. The defocusing of collector #12 has also been compared to test data when run with superheated steam (e.g. for July 17, 2013) and again shows very good agreement (not shown in this paper). Thus, single-phase flow is reproduced very well by the DFEM such that we can now concentrate on the complete loop configured in once-through mode. During all presented experiments, the pressure was kept constant at the outlet of the loop and effective irradiation did not vary significantly.

The DFEM configuration with the same lengths, same number of elements and all other parameters being kept constant is used for the following validation. Only optical efficiencies are adapted, if soiling occurred or reflectance changed notably, respectively. The same optical efficiencies are also applied to the MBM, if both models are compared. The main variable of interest is the temperature at the loop outlet. The variation of the end of evaporation is not shown explicitly here, but its dynamic behavior is well approximated as mirrored behavior of the outlet temperature, e.g. an increase in outlet temperature corresponds to a decrease/upstream-shift of the end of evaporation in the loop.

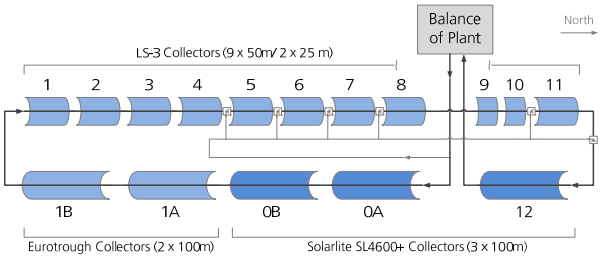

Fig. 2. Diagram of the new DISS test facility in once-through mode with optional injection lines; first collector #0A, last collector #12 ((Feldhoff, sp2013)).

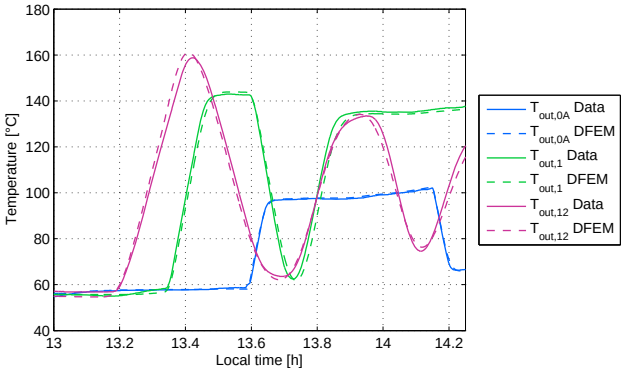

Fig. 3. Validation of water flow through complete loop with DFEM compared to data of June 18, 2013; DNI around 950 W/m², collectors in focus: #2 to #7 at 13.0h-13.25h, coll. #1A to #1B at 13.3h-13.55h, coll. #0A to #0B at 13.6h-14.14h.

The influence of the injector before collector 12 (used as injection B in MBM) is shown in Fig. 4. Both DFEM and MBM show very good agreement with a slightly better dynamic by the DFEM. If the inlet mass flow is decreased as shown in Fig. 5, the DFEM again shows a very good agreement. The MBM reacts too early and the peak does not correspond well. However, the initial dynamic is met well and absolute deviations are still acceptable.

When collector 5 is defocused, we can see a slight non-minimum phase behavior in Fig 6. That means, that at first the temperature will increase after defocusing and reach a maximum (at about 14.2 h local time). This is due to the density change by the reduced heat input, which causes a lower velocity of the steam. In consequence, more heat can be transferred to the steam at the outlet which results in a higher temperature. Note that the pressure drop effect described in [19] is also a result of this density disturbance. After the residence time of the fluid between inlet of collector 5 and loop outlet, the temperature starts decreasing (14.2 h) and reaches its lower value at about 14.4 h. This density effect is reproduced by the DFEM, but with a smoother local maximum. The same can be seen for the refocusing of collector 5 beginning at 14.7 h in Fig. 6. The MBM does not show the same good agreement, because collector 5 is only a small part of the modelled section 4I (injection A = injector before coll. #6). The local or distributed character cannot be maintained and only the overall energetic behavior is reproduced.

The non-minimum phase behavior gets stronger, if the density disturbance is located further upstream to the loop inlet. This is shown for a disturbance of inlet temperature in Fig. 7. The DFEM shows a slightly faster and steeper response than the data. The MBM can locate the disturbance exactly and thus shows very good agreement with the data, which is even more exact than the DFEM curve. We can conclude that the dynamics are represented very well by the MBM, if the disturbance location is resolved by the model. Other input variations have been performed and validated, but are not included in this paper due to limited space.

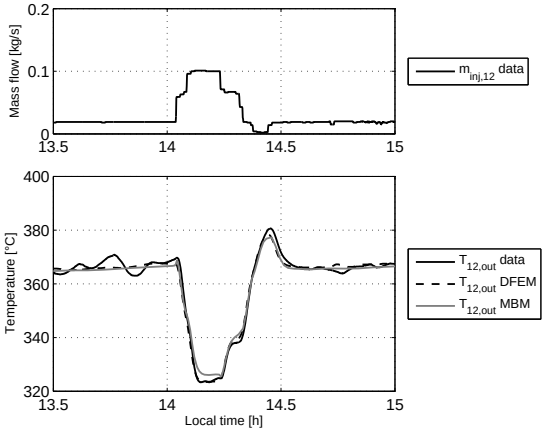

Fig. 4. Injection steps before collector #12 with DFEM and MBM compared to data of August 1, 2013.

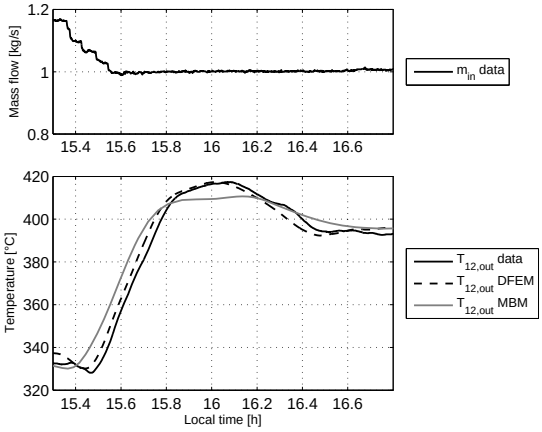

Fig. 5. Decrease of inlet mass flow with DFEM and MBM compared to data of July 25, 2013.

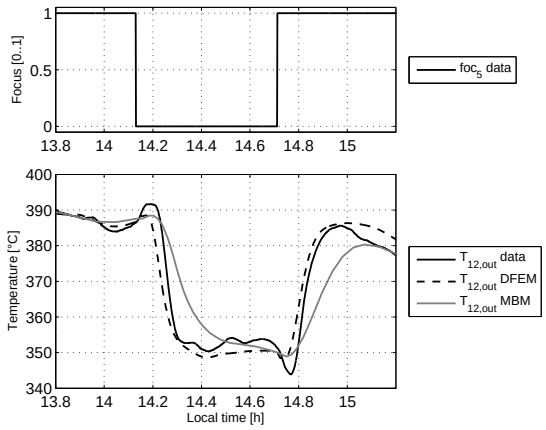

Fig. 6. De-/re-focusing of collector 5 with DFEM and MBM compared to data of July 26, 2013.

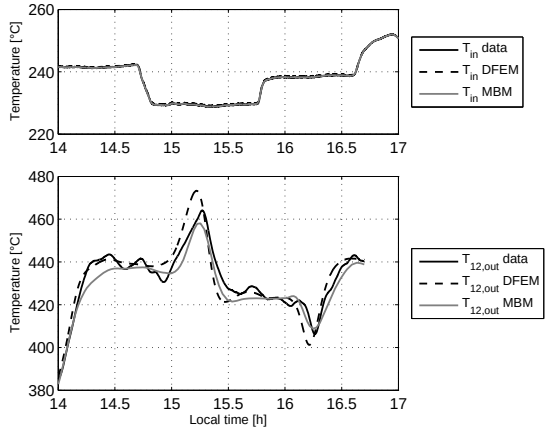

Fig. 7. Decrease and increase of inlet temperature with DFEM and MBM compared to data of August 9, 2013.

For designing control systems for OTM it is important to understand the characteristics of the system. When considering changes in mass flow we see smooth, delayed outlet temperature responses (compare Fig. 4 and 5). If density changes are stimulated by a disturbance (inlet temperature, local irradiation deviations), a first counter-response to the final steady state direction occurs. Control system theory would characterize this behavior as non-minimum phase. This effect reduces with the disturbance location further downstream as shown in Fig. 8 and vanishes completely for disturbances in the superheating section. Such a behavior is not notably discovered for pure single-phase flow loops with oil or molten salt, as the density differences are not that significant (density between inlet and outlet varies by a factor of about 20 for DSG loops). For start-up and first focus of an OTM loop this suggests starting with the first collector, while de-focusing should always start with the last collector.

Independent of the type of disturbance we find a strong dependency on the load situation (mass flow) which is common for most fluid dynamic systems, see Fig 9. For the control engineer, this means that a single set of control parameters is not sufficient to cover all operating conditions. Furthermore, the mass flow at the outlet cannot be influenced directly by the inlet mass flow, because the loop volume provides to some extent a buffer for liquid water. This must also be taken into account during controller design.

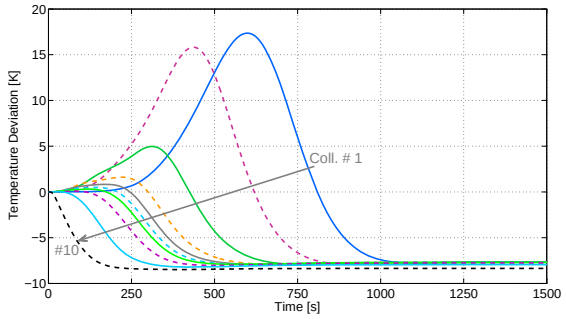

Fig. 8. Loop outlet temperature deviation caused by a DNI drop of 10 % on specified collector only for a 1500 m loop (10 collectors of 150 m each in series); based on DFEM.

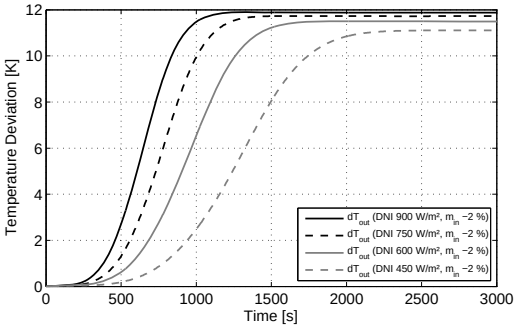

Fig. 9. Loop outlet temperature deviation caused by a decrease of inlet mass flow of -2 % for DISS facility at different operating/ irradiation conditions; based on DFEM.

4. Conclusions and outlook

This paper provides a general overview of transient OTM modeling and then presents two different types of OTM models. At first, DLR's discretized finite element model (DFEM) is described, which considers transient energy and mass balance, static momentum balance, and thermodynamic phase-equilibrium in the two-phase flow region. It can be used to study the characteristics of an OTM loop in detail and shows high accuracy in all transient situations. The second approach described is a moving boundary model (MBM) based on [21], which has been extended to meet the boundary conditions of the OTM in line focus solar steam generating systems. This model with concentrated parameters serves for fast predictions of the most relevant control variables, namely the outlet temperature and the location of the end point of evaporation. It can be used for various parameters or control design studies, and as core in a model predictive control algorithm.

It is shown that the response to local disturbances within the evaporation section cannot be reproduced well by the MBM. This limit must be considered when choosing the desired model. If irradiation can be considered the same on the whole solar collectors loop, the MBM offers clear computational advantages. If local effects shall be analyzed, transfer functions shall be derived or a detailed insight into the system characteristics is desired, the DFEM should be chosen.

Acknowledgements

The authors would like to thank the German Federal Ministry for Economic Affairs and Energy for the financial support given to the DUKE project under contract No. 0325293A. We also give special thanks to the operation and maintenance team of PSA's DISS test facility under supervision of Javier León.

References

[1] Feldhoff, J. F., Schmitz, K., Eck, M., Schnatbaum-Laumann, L., Laing, D., Ortiz-Vives, F., and Schulte-Fischedick, J. Comparative system analysis of direct steam generation and synthetic oil parabolic trough power plants with integrated thermal storage. Solar Energy, 86 (1), 2012, pp. 520-530.

[2] Hirsch, T., Eck, M., and Steinmann, W.-D. Simulation of transient two-phase flow in parabolic trough collectors using Modelica. 4th International Modelica Conference, Hamburg, Germany, 2005, pp. 403-412.

[3] Bonilla, J., Dormido, S., and Cellier, F. E. Switching Moving Boundary Modeals for Two-phase Flow Evaporators and Condensers. Communications in Nonlinear Science and Numerical Simulation, accepted manuscript (0), 2014.

[4] Ray, A., and Bowman, H. F. A Nonlinear Dynamic Model of a Once-Through Subcritical Steam Generator. Journal of Dynamic Systems, Measurement, and Control, 98 (3), 1976, pp. 332-339.

[5] Yebra, L. J., Berenguel, M., and Dormido, S. Extended moving boundary model for two phase flows. 16th IFAC World Congress, Prague, Czech Republic, 2005.

[6] Zapata, J. I., Pye, J., and Lovegrove, K. A transient model for the heat exchange in a solar thermal once through cavity receiver. Solar Energy, 93 (0), 2013, pp. 280-293.

[7] Feldhoff, J. F., Eickhoff, M., Karthikeyan, R., Krüger, J., León Alonso, J., Meyer-Grünefeldt, M., Müller, M., and Valenzuela Gutierrez, L. Concept comparison and test facility design for the analysis of direct steam generation in once-through mode. 18th SolarPACES Conference, Marrakech, Morocco, 2012.

[8] Zarza, E., Valenzuela, L., León, J., Hennecke, K., Eck, M., Weyers, H. D., and Eickhoff, M. Direct steam generation in parabolic troughs: Final results and conclusions of the DISS project. Energy, 29 (5-6), 2004, pp. 635-644.

[9] Feldhoff, J. F., Eickhoff, M., Keller, L., Alonso, J. L., Meyer-Grünefeldt, M., Valenzuela, L., Pernpeintner, J., and Hirsch, T. Status and First Results of the DUKE Project – Component Qualification of New Receivers and Collectors. Energy Procedia, 49 (2014), 2014, pp. 1766-1776.

[10] Barre, F., and Bernard, M. The CATHARE code strategy and assessment. Nuclear Engineering and Design, 124 (3), 1990, pp. 257-284.

[11] Bestion, D. The physical closure laws in the CATHARE code. Nuclear Engineering and Design, 124 (3), 1990, pp. 229-245.

[12] Sonnenburg, H. G., and Tuomisto, H. Analysis of a selected two-phase flow phenomenon in VVER reactors with horizontal steam generators. Nuclear Engineering and Design, 145 (1–2), 1993, pp. 261-269.

[13] Dimenna, R. A., Larson, J. R., Johnson, R. W., Larson, T. K., Miller, C. S., Streit, J. E., Hanson, R. G., and Kiser, D. M. RELAP5/MOD2 models and correlations. Technical Report NUREG/CR-5194; EGG-2531; ON: TI88016994, Idaho National Engineering Laboratory, Washington, DC, USA, 1988.

[14] Hoffmann, A., Merk, B., Hirsch, T., and Pitz-Paal, R. Simulation of thermal fluid dynamics in parabolic trough receiver tubes with direct steam generation using the computer code ATHLET. Kerntechnik, 79 (3), 2014, pp. 175-186.

[15] Lippke, F. Direct Steam Generation in Parabolic Trough Solar Power Plants: Numerical Investigation of the Transients and the Control of a Once-Through System. Journal of Solar Energy Engineering, 118 (1), 1996, pp. 9-14.

[16] Patankar, S., Numerical Heat Transfer and Fluid Flow, Taylor & Francis, 1980.

[17] Steinmann, W.-D., Dynamik solarer Dampferzeuger, Fortschritts-Berichte VDI, VDI-Verlag, Düsseldorf, Germany, 2001.

[18] Hirsch, T., Dynamische Systemsimulation und Auslegung des Abscheidesystems für die solare Direktverdampfung in Parabolrinnenkollektoren, Fortschritt-Berichte Energietechnik, Reihe 6, No. 535, VDI Verlag, Düsseldorf, Germany, 2005.

[19] Lobón, D. H., Valenzuela, L., and Baglietto, E. Modeling the dynamics of the multiphase fluid in the parabolic-trough solar steam generating systems. Energy Conversion and Management, 78 (0), 2014, pp. 393-404.

[20] Adams, J., Clark, D. R., Louis, J. R., and Spanbauer, J. P. Mathematical Modeling of Once-Through Boiler Dynamics. Power Apparatus and Systems, IEEE Transactions on, 84 (2), 1965, pp. 146-156.

[21] Ray, A. Dynamic modelling of once-through subcritical steam generator for solar applications. Applied Mathematical Modelling, 4 (6), 1980, pp. 417-423.

[22] Jensen, J. M. Dynamic Modeling of Thermo-Fluid Systems - With focus on evaporators for refrigeration. Technical University of Denmark, 2003.

[23] Jensen, J. M., and Tummescheid, H. Moving Boundary Models for dynamic simulations of two-phase Flows. 2nd International Modelica Conference, DLR, Oberpfaffenhofen, Germany, 2002, pp. 235-244.

[24] Morari, M., and Zafiriou, E., Robust Process Control, Prentice Hall, 1989.

[25] Profos, P., Die Regelung von Dampfanlagen, Springer, Berlin, 1962.

[26] Eck, M., Die Dynamik der solaren Direktverdampfung und Überhitzung in Parabolrinnenkollektoren, Fortschritts-Berichte VDI, VDI-Verlag, Düsseldorf, Germany, 2001.

[27] Koch, S., Hirsch, T., and Eck, M. 2007.

[28] Zunft, S., Dynamik und Regelung von Solarkollektorfeldern zur Prozeßwärme- und Stromerzeugung, Fortschritt Berichte Energieerzeugung, VDI-Verlag, Stuttgart, 2003.

[29] Valenzuela, L. Control Automatico de Plantas de Generacion Directa de Vapor con Colectores Solares Cilindro-Parabolicos. PhD Thesis, University of Almeria/ CIEMAT, Madrid, 2008.

[30] Valenzuela, L., Zarza, E., Berenguel, M., and Camacho, E. F. Direct steam generation in solar boilers - Using feedback to maintain conditions under uncontrollable solar radiation. Control Systems, IEEE, 24 (2), 2004, pp. 15-29.

[31] Valenzuela, L., Zarza, E., Berenguel, M., and Camacho, E. F. Control concepts for direct steam generation in parabolic troughs. Solar Energy, 78 (2), 2005, pp. 301-311.

[32] Müller-Steinhagen, H., and Heck, K. A simple friction pressure drop correlation for two-phase flow in pipes. Chem. Eng. Process, 20, 1986, pp. 297-308.

[33] Forristall, R. Heat Transfer Analysis and Modeling of a Parabolic Trough Solar Receiver Implemented in Engineering Equation Solver. Technical Report NREL/TP-550-34169, National Renewable Energy Laboratory, Golden, Colorado, USA, 2003.

[34] Vdi, VDI Heat Atlas, Springer, Berlin Heidelberg [u.a.], 2010.

[35] Winterton, R. H. S. Where did the Dittus Boelter equation come from? Int. J. Heat Mass Transfer, 41 (4-5), 1998, pp. 809-810.

[36] Chen, J. C. Correlations for boiling heat transfer to saturated fluids in convective flow. Ind. Engng Chem. Proc. Des. Dev., 5, 1966, pp. 322-329.

[37] Goebel, O., Wärmeübergang in Absorberrohren von Parabolrinnen-Solarkraftwerken, VDI Fortschrittsberichte, VDI, 1998.

[38] Gunger, K. E., and Winterton, R. H. S. A general correlation for flow boiling in tubes and annuli. Int. J. Heat and Mass Transfer, 29 (3), 1986, pp. 351-358.

[39] Odeh, S. D., Morrison, G. L., and Behnia, M. Modelling of parabolic trough direct steam generation solar collectors. Solar Energy, 62 (6), 1998, pp. 395-406.

[40] Hirsch, T., Feldhoff, J. F., Hennecke, K., and Pitz-Paal, R. Advancements in the Field of Direct Steam Generation in Linear Solar Concentrators—A Review. Heat Transfer Engineering, 35 (3), 2013, pp. 258-271.

[41] Morille, F. Modellerstellung für die prädiktive Regelung eines Parabolrinnenkraftwerks mit Direktverdampfung. Diploma thesis, Karlsruhe Institute of Technolgy and DLR, 2013.